Clim. Past Discuss., 7, 1113–1137, 2011
www.clim-past-discuss.net/7/1113/2011/
doi:10.5194/cpd-7-1113-2011

Climate of the Past Discussions

The calcium-dust relationship in high-resolution data from Dome C, Antarctica

F. Lambert[1,2,*], **M. Bigler**[1,2], **J. P. Steffensen**[3], **M. Hutterli**[4], **and H. Fischer**[1,2]

[1]Climate and Environmental Physics, Physics Institute, University of Bern, Sidlerstrasse 5, 3012 Bern, Switzerland
[2]Oeschger Centre for Climate Change Research, University of Bern, Bern, Switzerland
[3]Ice and Climate, Niels Bohr Institute, University of Copenhagen, Juliane Maries Vej 30, 2100 København Ø, Denmark
[4]Britisch Antarctic Survey, High Cross, Madingley Road, Cambridge, CB3 0ET, UK
[*]now at: Korea Ocean Research and Development Institute, Ansan, Korea

Received: 2 March 2011 – Accepted: 28 March 2011 – Published: 4 April 2011

Correspondence to: F. Lambert (lambert@kordi.re.kr)

Published by Copernicus Publications on behalf of the European Geosciences Union.

Abstract

Ice core data from Antarctica provide detailed insights into the characteristics of past climate, atmospheric circulation, as well as changes in the aerosol load of the atmosphere. We present high-resolution records of soluble calcium (Ca^{2+}), non-sea-salt soluble calcium ($nssCa^{2+}$), and insoluble mineral aerosol dust from the East Antarctic Plateau at a depth resolution of 1 cm, spanning the past 800 000 yr. The comparison shows that the ratio of ionic proxies such as Ca^{2+} (or $nssCa^{2+}$) to particulate dust aerosol is variable in time. Accordingly, the insoluble dust record is representative of large and small atmospheric particulate dust load changes and better suited to quantify the aerosol effect on the radiation balance in the past. In contrast soluble dust proxies such as Ca^{2+} and $nssCa^{2+}$ will underestimate this effect but may be better suited to quantify the deposition of chemically active Ca^{2+} or other soluble dust derived nutrients into the Southern Ocean. The correlation between $nssCa^{2+}$ and particulate dust is time dependent with high correlations during glacial and low correlation during interglacial times. The low correlation during warm times may be partly caused by changes in the soluble calcium content of dust particles, possibly due to a more acidic atmosphere during interglacials. The ratio of $nssCa^{2+}$ to dust is dependent on the dust concentration itself. A simple mixing of two dust end members for glacial and interglacial conditions with $nssCa^{2+}$ to dust ratios of 0.045 and approximately 0.3, respectively, can explain the overall temporal change in the $nssCa^{2+}$ to dust ratio over time.

1 Introduction

Atmospheric aerosol production, mobilization, long-range aeolian transport, and deposition respond to climatic changes (Fischer et al., 2007a,b; Legrand and Mayewski, 1997; Mahowald et al., 2006; Wolff et al., 2006). Dust and other aerosols affect radiative forcing through absorption and scattering of radiation (Murphy et al., 1998) and play a role as condensation nuclei (Sassen et al., 2003; Schwartz, 1996). The total

CPD
7, 1113–1137, 2011

atmospheric dust load, as well as physical (e.g. size, shape) and mineralogical characteristics are important factors for the radiative budget of the atmosphere (Bellouin et al., 2005; Tegen, 2003), and for the micronutrient supply to terrestrial and marine ecosystems (Fung et al., 2000; Röthlisberger et al., 2004).

Insoluble mineral dust particles (dust) and soluble ionic aerosol constituents, such as calcium (Ca^{2+}) and sodium (Na^{+}), are transported through the atmosphere also to remote Polar areas, like the Central East Antarctic Plateau (Fischer et al., 2007b; Wolff et al., 2006). As they are non-volatile species, they are irreversibly deposited onto the ice sheets (Legrand and Mayewski, 1997). Thus, they are regularly measured in Polar ice cores and allow for conclusions concerning climatic processes in the aerosol source region and during transport in the past. Moreover, the export of dust derived micronutrients (such as Fe) to the ocean represents a major micro-nutrient input, especially in high nutrient low chlorophyll regions such as the Southern Ocean (Martin et al., 1991).

Strontium and neodymium isotopic analysis identified Southern South America ($>32^{\circ}$ S) as the primary dust source for dust deposited onto the Antarctic ice sheet during recent glacial stages (Delmonte et al., 2004) with a possible Australian contribution during recent interglacials (Delmonte et al., 2008; Revel-Rolland et al., 2006), and a possible additional source in the Puna-Altiplano in Argentina during glacials (Delmonte et al., 2010; Gaiero, 2007). In contrast to particulate dust, Ca^{2+} has, apart from terrestrial, also marine sources (Bigler et al., 2006; Legrand and Mayewski, 1997). Although the marine aerosol ratio of Ca^{2+} to Na^{+} is well known (Bowen, 1979), few studies have investigated the continental Ca^{2+} to Na^{+} ratio of terrestrial aerosols from specific regions (i.e. Southern South America) (Bigler et al., 2006). However, these ratios are needed to calculate the exclusively terrestrial non-sea-salt calcium ($nssCa^{2+}$) based on Ca^{2+} and Na^{+} measurements.

Because Ca^{2+} (and Na^{+}) was more rapidly measurable at high resolution in Polar ice cores than dust so far, it has routinely been used uncorrected (Ca^{2+}) or corrected ($nssCa^{2+}$) as a proxy for dust deposited in Central Greenland (e.g. Fuhrer et al., 1999)

CPD
7, 1113–1137, 2011

or in Central Antarctica (e.g. Fischer et al., 2007a; Röthlisberger et al., 2002). Although some studies have investigated the Ca^{2+} to dust relationship in Greenland (Ruth et al., 2002; Steffensen, 1997), only limited work has been done for Antarctica (Ruth et al., 2008).

In this study we present the complete datasets and investigate the relationship between the calcium and insoluble dust records from the Dome C ice core at 1 cm resolution and spanning the past 800 000 yr, obtained in the frame of the European Project for Ice Coring in Antarctica (EPICA).

2 Methods

The EPICA Dome Concordia (EDC) ice core was drilled in East Antarctica (75°06′ S; 123°21′ E) and covers the last 800 000 yr (Jouzel et al., 2007). From a depth of 24.2 m down to 3200 m a Continuous Flow Analysis (CFA) system (Röthlisberger et al., 2000) was applied to measure, among others, insoluble dust particles and soluble Ca^{2+} and Na^{+}. The data gathered with this method have a nominal depth resolution of ∼1 cm taking dispersion in the CFA system already into account, which corresponds to a formal sub-annual temporal resolution at the top and to ∼25 yr at the bottom of the ice core.

For the ionic constituents the detection limit was about 0.2 ng g^{-1} for Ca^{2+} and 3 ng g^{-1} for Na^{+} (Bigler et al., 2006). The mean error for both Ca^{2+} and Na^{+} is estimated to be lower than ±10% (Bigler et al., 2006; Röthlisberger et al., 2000). The sea-salt (ss) and non-sea-salt (nss) contribution to Na^{+} and Ca^{2+} can be calculated using the system of linear equations

$$[\mathrm{ssNa^{+}}] = (R_t \times [\mathrm{Na^{+}}] - [\mathrm{Ca^{2+}}]) \times (R_t - R_m)^{-1}$$

and

$$[\mathrm{nssCa^{2+}}] = R_t \times ([\mathrm{Ca^{2+}}] - R_m \times [\mathrm{Na^{+}}]) \times (R_t - R_m)^{-1},$$

CPD
7, 1113–1137, 2011

with R_t and R_m being the terrestrial and the marine Ca^{2+}/Na^+ ratio, respectively (Bigler et al., 2006; Röthlisberger et al., 2002). Traditionally, the ratio R_m was assigned to the marine bulk sea water ratio of 0.038 and R_t to the average crust value of 1.78 (Bowen, 1979). However, other sources than sea spray, such as frost flowers, may have contributed significantly to the marine ion concentrations in Central East Antarctica (Wolff et al., 2006). Consequently, R_m was adjusted to 0.044 for Antarctic ice core data (Rankin et al., 2000). A recent study by Bigler et al. (2006) that estimated these ratios empirically using high-resolution CFA data from Dome C found $R_m = 0.043 \pm 9\%$ and $R_t = 1.06 \pm 8\%$ for the East Antarctic plateau. The lower R_t value probably reflects the local crustal composition in Southern South America. We used the updated Ca^{2+}/Na^+ values from (Bigler et al., 2006) in this study, although the difference only marginally affects the calculation of $nssCa^{2+}$ (in contrast to $ssNa^+$, not discussed here). Calcium and sodium data below the detection limit were discarded to reduce the noise at low concentrations. Negative values in the $nssCa^{2+}$ record were also discarded to avoid artefacts produced by exceptionally high sodium concentrations, as the ratios R_t and R_m are in principle only valid on average, and might not apply to single data points. Assuming an error of 10% for Ca^{2+}, Na^+, R_m, and R_t, the uncertainty of the $nssCa^{2+}$ record amounts to $0.2\,ng\,g^{-1}$ (29%) during interglacials and $5.4\,ng\,g^{-1}$ (11%) during glacial maxima.

An additional analytical concern may be the amount of additional Ca^{2+} being leached from particulate dust after the ice sample has been melted. This amount may be dependent on the acidity of the sample. However, the very good correspondence of Ca^{2+} concentrations measured by CFA and traditional ion chromatography (IC) (Ruth et al., 2008) excludes that this represents a significant effect. In case of IC measurements, the melted sample gets in contact with the acidic IC eluent, which would lead to a higher solution of Ca^{2+} from particulate dust if this were to be an important effect. Only for very low Ca^{2+} concentrations does the IC data divert to somewhat higher concentrations. However, this is due to the higher analytical blank of the discrete IC analyses. Accordingly, the CFA measurements can be regarded as reliable data of Ca^{2+} concentrations

CPD
7, 1113–1137, 2011

in ice core melt water. Note, that this does not exclude a potential temporal variation in Ca^{2+} leaching of dust aerosol during atmospheric transport!

Insoluble dust concentration and size distribution below 769.5 m (from 44 to 800 kyr BP) were measured by laser-absorption particle sensors and counters (Abakus from Klotz, Germany) (Ruth et al., 2003), in the following denoted as Bern dust data. The particle detection limit of these laser particle devices (LPD) is approximately 1 µm of equivalent spherical particle diameter. The upper measuring limit was set to 17.2 µm. Within this size range the LPD counts the number of particle in 32 different channels. The sum of all channels is then converted into an analogue voltage signal. In the Bern dust data this voltage signal was converted to number of particles per millilitre as described in Bigler (2004). The first 769.5 m were measured with a custom-made device from the University of Copenhagen featuring 4 channels only.

As discussed in Fujii et al. (2003), there is coincidence loss when counting particles with a LPD. Furthermore, the detection limit and the upper measuring limit of a LPD are not the same as for established Coulter Counter (CC) devices. This leads to an approx. 4 times lower counting efficiency of the LPD compared to the CC. In order to make the two data sets directly comparable, and because we only consider total dust concentrations but not size distribution, it is sufficient to fit the LPD measurements to CC data.

CC measurements were performed on discrete 7 cm long samples at least every 6 m, but mostly every 55 cm over the whole EDC ice core. CC data and method are described in detail in Delmonte et al. (2002). The CC particle detection limit is 0.7 µm (equivalent spherical particle diameter) and the upper measuring limit was set to 22 µm. The mass of particles was calculated from the volume, assuming spherical particles with a density of 2.5 g cm^{-3}. Based on at least three consecutive measurements per sample, the uncertainty for the CC is 2% for samples with high dust concentration, while some low concentration samples showed more pronounced scattering (up to 20%) (Delmonte et al., 2002).

CPD
7, 1113–1137, 2011

The lowest part of the ice core (below 3000 m) had many cracks and breaks bearing the risk of contamination with drill fluid, whereas the rest of the core up to the end of the brittle zone (at ~950 m) was essentially break free. Contamination with drill fluid falsifies both LPD and CC measurements. They caused either saturations of the LPD signal or were clearly recognisable based on unreasonably large size distribution data. In addition, the stratigraphy of the ice below 3190 m was disturbed and the climatic relevance of data collected in that part is doubtful (Jouzel et al., 2007). Therefore, only the data down to 3190 m depth are considered in this study.

To perform the fit of the LPD to the CC data we averaged the LPD data of all 7 cm sections where CC measurements were available. However, CC measurements were made mostly on samples taken directly at the beginning or at the end of 110 cm ice core pieces. LPD data is sometimes incomplete at the extremities of the core pieces, because the decontamination procedure often resulted in a 2–3 cm loss at the beginning and end of the continuously measured samples. We thus considered only those data where at least 6 cm of LPD data overlapped the 7 cm CC data. 273 and 522 sections match this condition for the Copenhagen and Bern datasets, respectively, both covering the whole concentration range. The Bern data shows a very good linear relationship of the logarithmic values of CC mass (in ng g^{-1}) and LPD data (in number of particles ml^{-1}) with $r^2 = 0.85$ (Fig. 1b). The conversion equation is

$$\mathrm{Log}_{10}(\mathrm{mass}) = 0.85 \times \mathrm{Log}_{10}(\mathrm{data}) - 1.14.$$

For the Copenhagen data, the best fit between the CC mass (in ng g^{-1}) and the LPD signal (in V) was found to be described by the relation

$$\log_{10}(\mathrm{mass}) = 1.83 \times \ln(\log_{10}(100 \times \mathrm{signal})) + 1.61$$

with an r^2 of 0.8 (Fig. 1a). Assuming an error of 20% and 2% for both CC and LPD raw data during interglacials and glacials, respectively, we can produce an estimate for the uncertainty of the LPD mass data. A linear weighted total least square fit that considers uncertainties in both the dependent and independent variables (Krystek and

CPD
7, 1113–1137, 2011

Anton, 2007), yielded interglacial errors of 12% and 16%, and glacial errors of 6% and 8% for the Bern and Copenhagen devices, respectively.

Finally, dust flux was calculated by multiplying the total mass concentration with the accumulation rate for Dome C (typically about 3 and 1.5 cm per year during warm and cold periods, respectively) derived from δ Deuterium measurements (Jouzel et al., 2007). However, the uncertainty of the flux values, which is mainly controlled by the error in the accumulation rate, is estimated to be up to 30% during glacial periods (Fischer et al., 2007b; Schwander et al., 2001). We therefore only consider concentrations for our calculations.

3 Results and discussion

Calcium and insoluble dust both follow the major climatic cycles with higher concentrations during cold times. Figure 2 shows the EDC dust, Ca^{2+}, and $nssCa^{2+}$ concentrations, both at 1 cm and 55 cm resolution on a depth scale. We record typical interglacial concentration values of 0.5–1 ng g^{-1} for $nssCa^{2+}$, 1–2 ng g^{-1} for Ca^{2+}, and 10 ng g^{-1} for insoluble dust. During glacial maxima, average insoluble dust concentrations increase by over two orders of magnitude, while Ca^{2+} and $nssCa^{2+}$ average concentrations increase by a factor of about 30 and 60, respectively. In comparison, there is a factor of about 60 and 150 between Greenland Last Glacial Maximum (LGM) and Holocene Ca^{2+} and insoluble dust concentrations, respectively (Steffensen, 1997).

To examine the relationship between Ca^{2+}, $nssCa^{2+}$, and insoluble dust, we use scatter plots with logarithmic values to account for the log-normal distribution of the data (Fig. 3). The relationship between the logarithmic values of Ca^{2+} and insoluble dust seems to be fairly linear with a slight s-shape (Fig. 3a). There is a good overall correlation with a coefficient of determination of $r^2 = 0.84$ (with significance level $p < 0.0001$). A slightly larger variability at lower values is probably due to the higher measurement uncertainty close to the detection limit.

CPD
7, 1113–1137, 2011

The nssCa^{2+} to insoluble dust scatter plot (Fig. 3b) shows more variability, and the linear relationship between the logarithmic values of the two is a little worse than for Ca^{2+} with $r^2 = 0.79$ ($p < 0.0001$). This is to be expected since the Na^+ concentration used for the sea salt correction has an analytical uncertainty of 5–10% itself. The s-shape seems to be present here as well, although slightly hidden by the larger scatter at low concentration values. Discrepancies between Ca^{2+} and nssCa^{2+} are mostly related to low concentrations. The lower correlation between nssCa^{2+} and insoluble dust at these values is very probably an effect of the larger error due to the combined uncertainties of Ca^{2+} and Na^+ measurements close to the detection limit (see error bars in Fig. 3). Variations in R_m may also affect low nssCa^{2+} concentrations. The difference between a pure sea water source and a pure frost flower source would change the nssCa^{2+} calculation by 15% during interglacials (the difference is negligible during glacials). The more numerous small values in nssCa^{2+} also account for the slightly steeper slope in the dust-nssCa^{2+} relationship and reflect the important relative amount of sea-salt Ca^{2+} (ssCa^{2+}) during interglacials.

It is difficult to asses which proxy is the best to quantify atmospheric dust load variability. Due to its small error, the Ca^{2+} data may be well suited to study atmospheric dust load variations during glacials. During interglacials, the high percentage of marine Ca^{2+} prevents detailed conclusions on dust. The large error in nssCa^{2+} during warm times, and the fact that the ratios R_t and R_m are only average values, makes this dataset unsuited for detailed interglacial analysis. However, since the ssCa^{2+} contribution has been removed, it is more representative of glacial-interglacial changes than the Ca^{2+} data. The advantage of the insoluble dust data is that they combine a relatively small error throughout the dataset with a reliable estimate of glacial-interglacial changes in changes in the atmospheric dust aerosol load. Accordingly, to assess the influence of dust on the radiative forcing in the Southern Ocean region based on the EPICA ice core dust records over the last 800 000 yr, particulate dust aerosol appears to be better suited. Note, however, that the particulate dust load may not be so representative for the supply of biological or chemically active micronutrients into the ocean. Here, the

CPD
7, 1113–1137, 2011

amount of these micronutrients leached during transport or when the aerosol is entering the surface water is important. In fact significant changes between particulate dust and Ca^{2+} can be seen in our data (see below) and variations have also been measured in the iron record on the EPICA Dome C ice core, which are not seen in the Ca^{2+} or particulate dust records (Lambert et al., 2008; Wolff et al., 2006).

A more detailed examination of the temporal evolution of the dust-calcium coefficient of determination and ratio are displayed in Fig. 4a,b (Ca^{2+}/dust relations are displayed in black, whereas $nssCa^{2+}$/dust relations are displayed in grey), along with 1000 year median values of dust flux (Fig. 4c). The coefficients of determination were calculated in a 900 yr running window, between logarithmic 100 year median concentration data, that were high-pass filtered with a cut-off period of 15 kyr to eliminate the correlation induced by orbital frequencies (Fig. 4a). The ratio was calculated between 100 year median concentration values (Fig. 4b). Both datasets displayed are smoothed by a 25 point running average window for better visibility. There seem to be two distinct modes, one with high correlation ($r^2 > 0.6$, $p < 0.0001$) between insoluble dust and calcium, and one with rather low correlation between the two ($r^2 < 0.2$, $p < 0.0001$). The periods with low correlation correspond to interglacial periods, whereas highly correlated periods occur during glacial maxima. The very low coefficient of determination during warm times illustrates to what point the insoluble dust and the Ca^{2+} and $nssCa^{2+}$ data differ in those sections. The marine contribution to Ca^{2+} and the relatively large error of $nssCa^{2+}$ at low values partly explain this. However, the discrepancy between the two datasets during warm times could also be an effect of highly variable Ca^{2+}/dust ratios of the dust generated in the source areas or variable mixing of different dust sources. Also a variable but more acidic atmosphere than during cold times could add to this decorrelation. The enhanced oxidative potential of the atmosphere during interglacials could have contributed soluble Ca^{2+} from otherwise insoluble calcium containing minerals (feldspars, clay) in airborne dust particles. This would have significantly changed the original composition, independently of the conditions that were in effect at the dust source.

CPD
7, 1113–1137, 2011

It is interesting to note, that during the oldest 200 kyr, the dust-calcium correlation has a markedly different pattern than in the time since 600 000 yr BP. The calcium to insoluble dust ratio (Fig. 4b) also changes its pattern after 700 000 yr BP. Taken at face value, these changes in the bottom part of the core point to a change in the crustal composition of dust transported to Antarctica during the climatic reorganisation that happened at the Mid-Pleistocene Revolution. Note, however, that in this depth interval, single dust particles were agglomerated, possibly due to ice recrystallization and shear deformation processes. This could potentially affect the leaching of Ca^{2+} from these aggregates.

The EDC Ca^{2+} to insoluble dust ratio fluctuates between about 0.04 and 0.3 (Fig. 4b), and is much higher than the ratio that was measured in Greenland (between 0.005 and 0.015; Steffensen, 1997). This difference may be due to different mineral composition of dust transported to Northern or Southern Polar region. Alternatively, Greenland dust may have been subjected to a greater amount of Ca^{2+} leaching on the way from its source in Eastern Asia than Antarctic dust. The $nssCa^{2+}$ to insoluble dust ratio ranges between about 0.04 and 0.2, although the fluctuations are generally smaller than those in the Ca^{2+}/dust ratio. Low and high Antarctic ratios are related to glacial maxima and interglacials, respectively. This is consistent with finding from Steffensen (1997) who found the calcium-dust ratio in Greenland to be correlated to concentration. The size of dust particles is unlikely to have played a role, as it stays fairly constant over the record, with glacial-interglacial changes of only 5% (Delmonte et al., 2004; Lambert et al., 2008). The similar findings in Greenland and Antarctic data, as well as the fact that the $nssCa^{2+}$ to insoluble dust ratio shows a similar variability pattern than the Ca^{2+} to insoluble dust ratio, suggest that varying amounts of sea-salt calcium were not responsible for these changes.

How can we explain the temporal variation in the $nssCa^{2+}$/dust ratio? If we assume that we have typical $nssCa^{2+}$/dust ratios for interglacial dust (be aware that this could potentially include additional calcium from the more acidic atmosphere during warm times, and may not necessarily reflect the ratio at the source) and for dust deposited

CPD
7, 1113–1137, 2011

in Antarctica during glacials, we can explain the change in the nssCa^{2+}/dust ratio as displayed in Fig. 5a as a mixing of the two end members with different nssCa^{2+}/dust ratios. An easy mass balance leads to

$$\left(\frac{\text{nss}Ca^{2+}}{\text{dust}}\right)_{\text{measured}} = \left(\frac{\text{nss}Ca^{2+}}{\text{dust}}\right)_{\text{glacial}} + \left(\left(\frac{\text{nss}Ca^{2+}}{\text{dust}}\right)_{\text{interglacial}} - \left(\frac{\text{nss}Ca^{2+}}{\text{dust}}\right)_{\text{glacial}}\right)\frac{\text{dust}_{\text{interglacial}}}{\text{dust}_{\text{measured}}}$$

with $\text{dust}_{\text{interglacial}}$ being the amount of particulate dust derived from the interglacial dust source contributed to the total measured dust concentration $\text{dust}_{\text{measured}}$. Accordingly, a linear relationship between the measured nssCa^{2+}/dust ratio with the inverse of the measured dust concentration is expected. Using linear regression of such a linear relationship with $1/\text{dust}_{\text{measured}}$ for a 100 yr average data set over the entire 800 000 yr, the nssCa^{2+}/dust ratio of the glacial end member can be determined from the *y*-intercept as 0.045 (Fig. 5b). The slope of the regression is 1.24, which leads to a measured nssCa^{2+}/dust ratio of about 0.2–0.3 for the lowest (interglacial) dust concentrations. The scatter of the data around the hyperbola is quite large and accordingly the coefficient of determination of the regression is only 0.17.

Interestingly, there is one time interval where the data points clearly deviate from this overall behaviour during Marine Isotope Stage 16 (time interval 645–670 kyr BP). In this time interval (red points in Fig. 5a) the interglacial nssCa^{2+}/dust ratio is already reached at much higher total dust concentrations. The linear regression over 1/dust for this time interval in our 100 yr average dataset leads to a glacial end member ratio of again 0.046 but a slope of 14.69. The final (interglacial) nssCa^{2+} ratios reached are again at around 0.3. Based on our simple mixing approach, this implies that the dust contribution from the interglacial dust source was about 12 times higher during this time than for other interglacials. This deviation of the Ca^{2+}/dust ratio on dust concentration during MIS 16 is surprising. Although marine oxygen isotope data record exceptionally high values during MIS 16 (Lisiecki and Raymo, 2005), this glacial period does not stand out in various climate parameters of the Dome C ice core (stable water isotopes, greenhouse gases, aerosol concentrations). Checking our CFA LPD data,

CPD
7, 1113–1137, 2011

we could not find a problem with our working procedure, thus making a measurement artefact unlikely. However, a comparison of the LPD data with the very few CC dust values available for this time interval, points to an underestimation of the LPD dust concentration. Such an unexplained systematic error would lead to an overestimation of the Ca^{2+}/dust ration in this interval. Accordingly, the anomalous relationship of the Ca^{2+}/dust ratio on dust concentration in this interval has to be taken with caution.

Another difference can be observed when comparing long glaciations with rather short deglaciations in our mixing diagram (for example for the time window from MIS 7.1 to MIS 5.5, see Fig. 6). Here it becomes clear that the nssCa^{2+}/dust ratio is slightly higher for the deglaciation (dark blue dots, 130–145 kyr BP) compared to intermediate dust concentrations (green to yellow dots, 160–180 kyr BP). Nevertheless they both end in the same glacial and interglacial end members with a nssCa^{2+}/dust ratio of about 0.3 and 0.045 and similar glacial and interglacial total dust concentrations. Again, according to the equation above this implies that during deglaciations the relative contributions of the interglacial dust source to the total dust concentration was higher. We speculate that during deglaciations, an excess of "interglacial" dust was liberated at the source. This may potentially be linked to the retreat of glaciers in the South American source region during the deglaciation that may lead to a stronger interglacial dust source at that time.

The long-term temporal variations in the calcium to insoluble dust ratio either reflect a variable leaching of dust aerosol during glacial and interglacial conditions during aerosol transport or a different Ca^{2+} content of the dust aerosol produced at the source. At least the general trend that can be explained by mixing of an interglacial and a glacial end member points to the latter. This could be related to an additional dust input from Australian or even local Antarctic sources during interglacials that becomes insignificant relative to the total dust deposition during glacial times, but potentially also to a change in the weathering conditions from glacials to interglacials in Patagonian dust source regions. Interestingly, a clear change in dust composition has been also derived from He isotopic measurements on mineral dust aerosol on the EPICA Dronning

CPD
7, 1113–1137, 2011

Maud Land ice core between the last glacial and the Holocene (Winckler and Fischer, 2006). In contrast, the marine contribution to Ca^{2+}, i.e. R_m is relatively well constrained around 0.04, and although varying contributions from open water and frost flowers can explain some of the variability in the interglacial $nssCa^{2+}$ record, the difference is not large enough to explain the changes in the calcium to insoluble dust ratio.

4 Conclusions

The EDC soluble calcium, non-sea-salt calcium and insoluble dust records of the past 800 000 yr have been processed and calibrated, and are presented in their full 1 cm resolution. The calcium and insoluble dust particle concentrations evolve in parallel, with Ca^{2+} and $nssCa^{2+}$ increasing from interglacials to glacial maxima by a factor of about 30 and 60, respectively, while insoluble dust concentrations increase by over two orders of magnitudes.

The Ca^{2+} data have a small analytical uncertainty but its variations would underestimate changes in the atmospheric dust load, which are important to assess the effect of dust aerosol changes on the radiative balance. In addition, the important relative contribution from $ssCa^{2+}$ during warm times makes Ca^{2+} generally a poorer proxy for atmospheric dust during interglacials. The relatively high error in the $nssCa^{2+}$ calculation limits its use to quantify dust variability at all times, but it is better suited than the Ca^{2+} record when estimating glacial-interglacial changes. The insoluble dust record appears to be most indicated to study atmospheric dust load variations, as well as glacial-interglacial changes, although one must keep its uncertainty in mind. On the other hand, leachable Ca^{2+} is the better proxy for aeolian Ca^{2+} input into the Ocean, which has an influence on the alkalinity of the ocean water.

Both Ca^{2+} and $nssCa^{2+}$ show a high correlation with insoluble dust during glacials and a low correlation during interglacials. The low interglacial correlation can partly be explained by the large marine contribution to total Ca^{2+} and the substantial error in $nssCa^{2+}$ at low values. In addition, it may be due to an input of dust with variable

CPD
7, 1113–1137, 2011

Ca^{2+}/dust ratios from different source regions or influenced by the effect of a more acidic atmosphere during warm times. The latter would add a contribution of soluble Ca^{2+} from otherwise insoluble calcium containing minerals in dust particles, which would be relatively independent from the dust source conditions.

The calcium to insoluble dust ratio varies by up to a factor of 6 between glacials and interglacials, with higher values during interglacials. The changes can be attributed mostly to variations in the Ca^{2+}/dust ratio of glacial and interglacial dust particles. These variations could be a result of the additional soluble Ca^{2+} leached by the more acidic atmosphere during warm times, or from different Ca^{2+}/dust ratios of the dust sources during both time intervals, However, the overall temporal change in the Ca^{2+}/dust ratios can generally be explained by a mixing of two glacial and interglacial dust end members with different Ca^{2+}/dust ratio, with the strength of the interglacial dust contribution apparently varying between different time intervals over the last 800 000 yr.

Acknowledgements. This work is a contribution to the European Project for Ice Coring in Antarctica (EPICA), a joint European Science Foundation/European Commission (EC) scientific programme, funded by the EU (EPICA-MIS) and by national contributions from Belgium, Denmark, France, Germany, Italy, The Netherlands, Norway, Sweden, Switzerland and the UK. The main logistic support at Dome C was provided by IPEV and PNRA. We thank all the persons involved in the fieldwork to obtain the comprehensive data set. Fabrice Lambert is supported by KORDI (PE 9853A, PE 98651).

References

Bellouin, N., Boucher, O., Haywood, J., and Reddy, M. S.: Global estimate of aerosol direct radiative forcing from satellite measurements, Nature, 438, 1138–1141, 2005.

Bigler, M.: Hochauflösende Spurenstoffmessungen an polaren Eisbohrkernen: glaziochemische und klimatische Prozessstudien, Ph.D. thesis, University of Bern, Bern, Switzerland, 2004.

CPD
7, 1113–1137, 2011

Bigler, M., Röthlisberger, R., Lambert, F., Stocker, T. F., and Wagenbach, D.: Aerosol deposited in East Antarctica over the last glacial cycle: detailed apportionment of continental and sea-salt contributions, J. Geophys. Res., 111, 1–14, 2006.

Bowen, H. J. M.: Environmental Chemistry of the Elements, Academic Press, London, 1979.

Delmonte, B., Petit, J. R., and Maggi, V.: Glacial to Holocene implications of the new 27,000-year dust record from the EPICA Dome C (East Antarctica) ice core, Clim. Dynam., 18, 647–660, 2002.

Delmonte, B., Basile-Doelsch, I., Petit, J.-R., Maggi, V., Revel-Rolland, M., Michard, A., Jagoutz, E., and Grousset, F.: Comparing the Epica and Vostok dust records during the last 220,000 years: stratigraphical correlation and provenance in glacial periods, Earth-Sci. Rev., 66, 63–87, 2004.

Delmonte, B., Andersson, P. S., Hansson, M., Schöberg, H., Petit, J. R., Basile-Doelsch, I., and Maggi, V.: Aeolian dust in East Antarctica (EPICA-Dome C and Vostok): provenance during glacial ages over the last 800 kyr, Geophys. Res. Lett., 35, 2–7, 2008.

Delmonte, B., Andersson, P. S., Schöberg, H., Hansson, M., Petit, J. R., Delmas, R., Gaiero, D. M., Maggi, V., and Frezzotti, M.: Geographic provenance of aeolian dust in East Antarctica during Pleistocene glaciations: preliminary results from Talos Dome and comparison with East Antarctic and new Andean ice core data, Quaternary Sci. Rev., 29, 256–264, 2010.

Fischer, H., Fundel, F., Ruth, U., Twarloh, B., Wegner, A., Udisti, R., Becagli, S., Castellano, E., Morganti, A., and Severi, M.: Reconstruction of millennial changes in dust emission, transport and regional sea ice coverage using the deep EPICA ice cores from the Atlantic and Indian Ocean sector of Antarctica, Earth Planet. Sc. Lett., 260, 340–354, 2007a.

Fischer, H., Siggaard-Andersen, M. L., Ruth, U., Röthlisberger, R., and Wolff, E. W.: Glacial/interglacial changes in mineral dust and sea-salt records in Polar ice cores: sources, transport, and deposition, Rev. Geophys., 45(26), RG1002, doi:10.1029/2005RG000192, 2007b.

Fuhrer, K., Wolff, E. W., and Johnsen, S. J.: Timescales for dust variability in the Greenland Ice Core Project(GRIP) ice core in the last 100 000 years, J. Geophys. Res., 104, 31043–31052, 1999.

Fujii, Y., Kohno, M., Matoba, S., Motoyama, H., and Watanabe, O.: A 320 k-year record of microparticles in the Dome Fuji, Antarctica ice core measured by laser-light scattering, Mem. Natl. Inst. Polar Res., 57, 46–62, 2003.

CPD
7, 1113–1137, 2011

Fung, I. Y., Meyn, S. K., Tegen, I., Doney, S. C., John, J. G., and Bishop, J. K. B.: Iron supply and demand in the upper ocean, Global Biogeochem. Cy., 14, 281–295, 2000.
Gaiero, D. M.: Dust provenance in Antarctic ice during glacial periods: from where in Southern South America?, Geophys. Res. Lett., 34, 1–6, 2007.
Jouzel, J., Masson-Delmotte, V., Cattani, O., Dreyfus, G., Falourd, S., Hoffmann, G., Minster, B., Nouet, J., Barnola, J. M., Chappellaz, J., Fischer, H., Gallet, J. C., Johnsen, S., Leuenberger, M., Loulergue, L., Luethi, D., Oerter, H., Parrenin, F., Raisbeck, G., Raynaud, D., Schilt, A., Schwander, J., Selmo, E., Souchez, R., Spahni, R., Stauffer, B., Steffensen, J. P., Stenni, B., Stocker, T. F., Tison, J. L., Werner, M., and Wolff, E. W.: Orbital and millennial Antarctic climate variability over the past 800,000 years, Science, 317, 793–796, 2007.
Krystek, M. and Anton, M.: A weighted total least-squares algorithm for fitting a straight line, Meas. Sci. Technol., 18, 3438–3442, 2007.
Lambert, F., Delmonte, B., Petit, J. R., Bigler, M., Kaufmann, P. R., Hutterli, M. A., Stocker, T. F., Ruth, U., Steffensen, J. P., and Maggi, V.: Dust-climate couplings over the past 800,000 years from the EPICA Dome C ice core, Nature, 452, 616–619, 2008.
Legrand, M. and Mayewski, P.: Glaciochemistry of Polar ice cores: a review, Rev. Geophys., 35, 219, 1997.
Lisiecki, L. E. and Raymo, M. E.: A Pliocene-Peistocene stack of 57 globally distributed benthic δ^{18}O records, Paleoceanography, 20(1), PA1003, doi:10.1029/2004PA001071, 2005.
Mahowald, N. M., Yoshioka, M., Collins, W. D., Conley, A. J., Fillmore, D. W., and Coleman, D. B.: Climate response and radiative forcing from mineral aerosols during the last glacial maximum, pre-industrial, current and doubled-carbon dioxide climates, Geophys. Res. Lett., 33, 2–5, 2006.
Martin, J. H., Gordon, R. M., and Fitzwater, S. E.: The case for iron, Limnol. Oceanogr., 36, 1793–1802, 1991.
Murphy, D. M., Brechtelk, F. J., Kreidenweisk, S. M., and Po, M.: Influence of sea-salt on aerosol radiative properties in the Southern Ocean marine boundary layer, Nature, 392, 62–65, 1998.
Rankin, A. M., Auld, V., and Wolff, E. W.: Frost flowers as a source of fractionated sea salt aerosol in the Polar regions, Geophys. Res. Lett., 27, 3469, 2000.

CPD
7, 1113–1137, 2011

Revel-Rolland, M., Dedeckker, P., Delmonte, B., Hesse, P., Magee, J., Basiledoelsch, I., Grousset, F., and Bosch, D.: Eastern Australia: a possible source of dust in East Antarctica interglacial ice, Earth Planet. Sc. Lett., 249, 1–13, 2006.

Röthlisberger, R., Bigler, M., Hutterli, M., Sommer, S., Stauffer, B., Junghans, H. G., and Wagenbach, D.: Technique for continuous high-resolution analysis of trace substances in firn and ice cores, Environ. Sci. Technol., 34, 338–342, 2000.

Röthlisberger, R., Mulvaney, R., Wolff, E. W., Hutterli, M. A., Bigler, M., Sommer, S., and Jouzel, J.: Dust and sea salt variability in Central East Antarctica (Dome C) over the last 45 kyrs and its implications for southern high-latitude climate, Geophys. Res. Lett., 29, 1–5, 2002.

Röthlisberger, R., Bigler, M., Wolff, E. W., Joos, F., Monnin, E., and Hutterli, M. A.: Ice core evidence for the extent of past atmospheric CO_2 change due to iron fertilisation, Geophys. Res. Lett., 31, 2–5, 2004.

Ruth, U., Wagenbach, D., Bigler, M., Steffensen, J. P., Röthlisberger, R., and Miller, H.: High resolution microparticle profiles at NGRIP: case studies of the calcium-dust relationship Peer reviewed article, Ann. Glaciol., 35, 237–242, 2002.

Ruth, U., Wagenbach, D., Steffensen, J. P., and Bigler, M.: Continuous record of microparticle concentration and size distribution in the Central Greenland NGRIP ice core during the last glacial period, J. Geophys. Res., 108, 1–12, 2003.

Ruth, U., Barbante, C., Bigler, M., Delmonte, B., Fischer, H., Gabrielli, P., Gaspari, V., Kaufmann, P., Lambert, F., Maggi, V., Marino, F., Petit, J.-R., Udisti, R., Wagenbach, D., Wegner, A., and Wolff, E. W.: Proxies and measurement techniques for mineral dust in Antarctic ice cores, Environ. Sci. Technol., 42, 5675–5681, 2008.

Sassen, K., Demott, P. J., Prospero, J. M., and Poellot, M. R.: Saharan dust storms and indirect aerosol effects on clouds: CRYSTAL-FACE results, Geophys. Res. Lett., 30, 1–4, 2003.

Schwander, J., Jouzel, J., Hammer, C. U., Petit, J. R., Udisti, R., and Wolff, E. W.: A tentative chronology for the EPICA Dome Concordia ice core, Geophys. Res. Lett., 28, 4243–4246, 2001.

Schwartz, S. E.: The whitehouse effect-shortwave radiative forcing of climate by anthropogenic aerosols: an overview, J. Aerosol. Sci, 27, 359–382, 1996.

Steffensen, J. P.: The size distribution of microparticles from selected segments of the Greenland ice core project ice core representing different climatic periods, J. Geophys. Res.-Oceans, 102, 26, 1997.

CPD
7, 1113–1137, 2011

Tegen, I.: Modeling the mineral dust aerosol cycle in the climate system, Quaternary Sci. Rev., 22, 1821–1834, 2003.

Winckler, G. and Fischer, H.: 30,000 years of cosmic dust in Antarctic ice, Science, 313, 491, 2006.

Wolff, E. W., Fischer, H., Fundel, F., Ruth, U., Twarloh, B., Littot, G. C., Mulvaney, R., Röthlisberger, R., de Angelis, M., Boutron, C. F., Hansson, M., Jonsell, U., Hutterli, M. A., Lambert, F., Kaufmann, P., Stauffer, B., Stocker, T. F., Steffensen, J. P., Bigler, M., Siggaard-Andersen, M. L., Udisti, R., Becagli, S., Castellano, E., Severi, M., Wagenbach, D., Barbante, C., Gabrielli, P., and Gaspari, V.: Southern Ocean sea-ice extent, productivity and iron flux over the past eight glacial cycles, Nature, 440, 491–496, 2006.

CPD

7, 1113–1137, 2011

The calcium-dust relationship in high-resolution data from Dome C

F. Lambert et al.

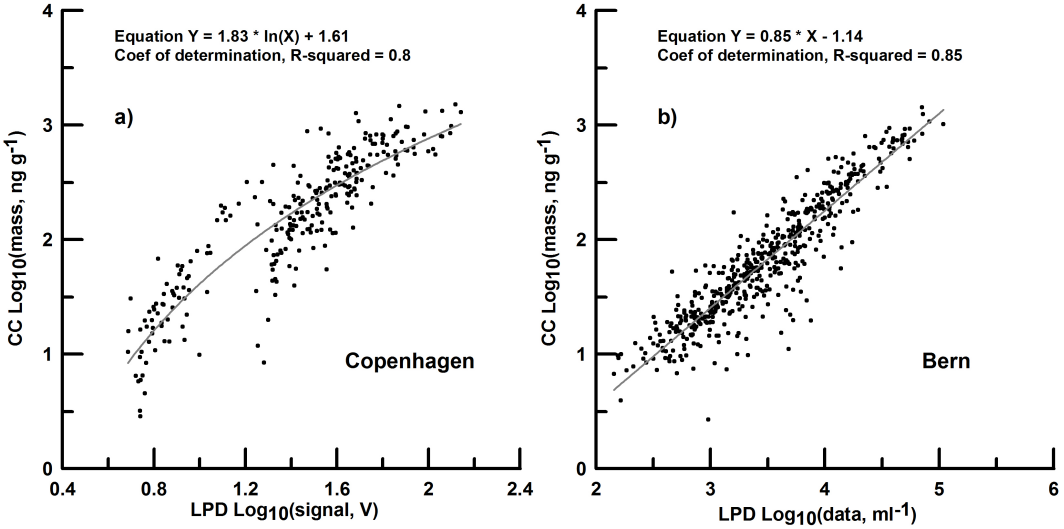

Fig. 1. Calibration fit between logarithmic values of the Copenhagen **(a)** and Bern **(b)** LPD signal, and logarithmic mass concentration measured by CC.

CPD
7, 1113–1137, 2011

The calcium-dust relationship in high-resolution data from Dome C

F. Lambert et al.

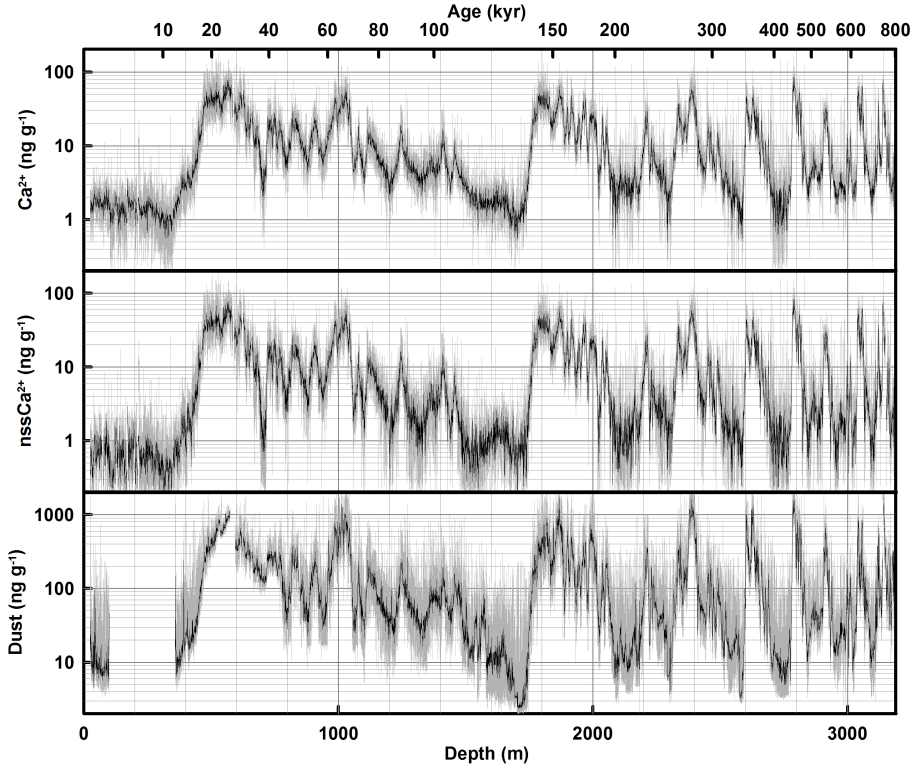

Fig. 2. Calcium, non-sea-salt calcium, and dust concentration values at 1 cm resolution (grey), overlaid with 55 cm mean values (black) from EPICA Dome C CFA on the depth scale. The EDC3 time-scale in kyr is indicated on top. Dust was not measured between 100 and 358 m depth.

CPD
7, 1113–1137, 2011

The calcium-dust relationship in high-resolution data from Dome C

F. Lambert et al.

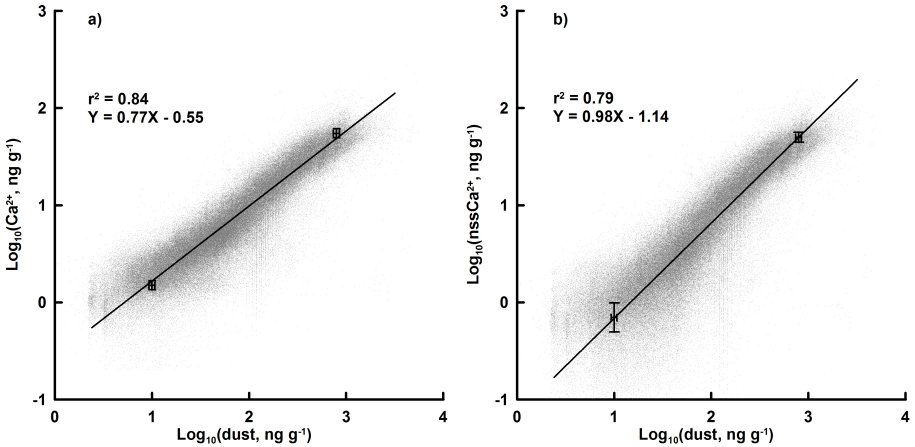

Fig. 3. Logarithmic values of Ca^{2+} **(a)** and $nssCa^{2+}$ **(b)** concentrations plotted against the logarithmic values of dust concentration, with error bars at average interglacial and glacial maximum levels. A two-sided regression yields overall correlation coefficients of $r^2 = 0.84$ and $r^2 = 0.79$, respectively. The dataset holds over 260 000 data points. The apparent vertical lines in the scatter are due to coarse rounding in the Copenhagen dust data.

CPD
7, 1113–1137, 2011

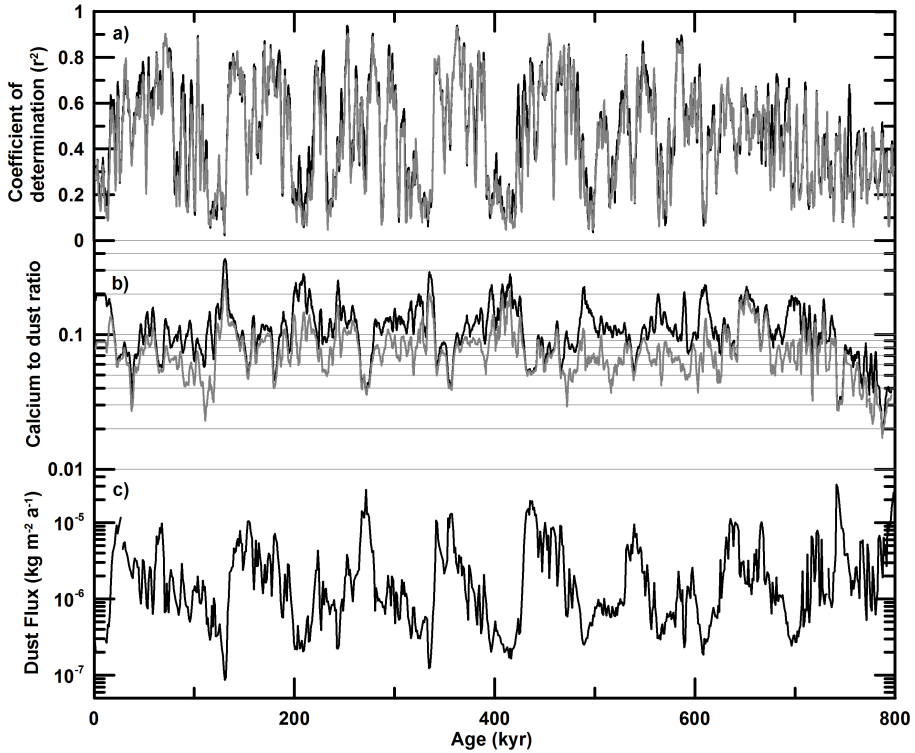

Fig. 4. **(a)** Coefficient of determination r^2 between the high-pass filtered (cut-off frequency of 15 kyr) logarithmic values of Ca^{2+} and dust (in black), and of $nssCa^{2+}$ and dust (in grey) concentrations, using 100 yr median values and a 900 yr gliding window (black). The data are presented smoothed by a 25 point running average window. **(b)** Ratio of Ca^{2+} and dust (in black), and $nssCa^{2+}$ and dust (in grey) concentrations, using 100 a median values, on a logarithmic scale. **(c)** Dust flux in kg m^{-2} yr^{-1} on a logarithmic scale.

CPD
7, 1113–1137, 2011

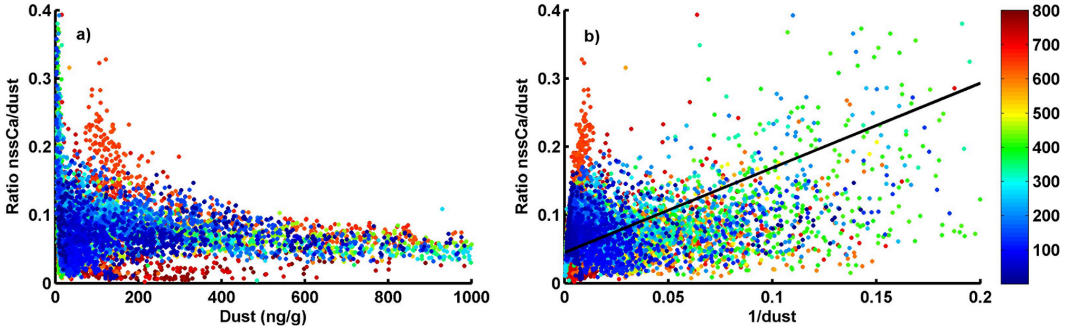

Fig. 5. (a) Scatter plot of the ratio nssCa^{2+}/dust versus dust concentration using 100 yr median data. **(b)** Scatter plot of the ratio nssCa^{2+}/dust versus the inverse of dust concentration using 100 yr median data. The black line represents the two sided linear regression with y-axis intercept 0.045 and slope 1.24 ($r^2 = 0.17$). The colour bar marks the age of the points in kyr BP for both plots.

CPD
7, 1113–1137, 2011

The calcium-dust relationship in high-resolution data from Dome C

F. Lambert et al.

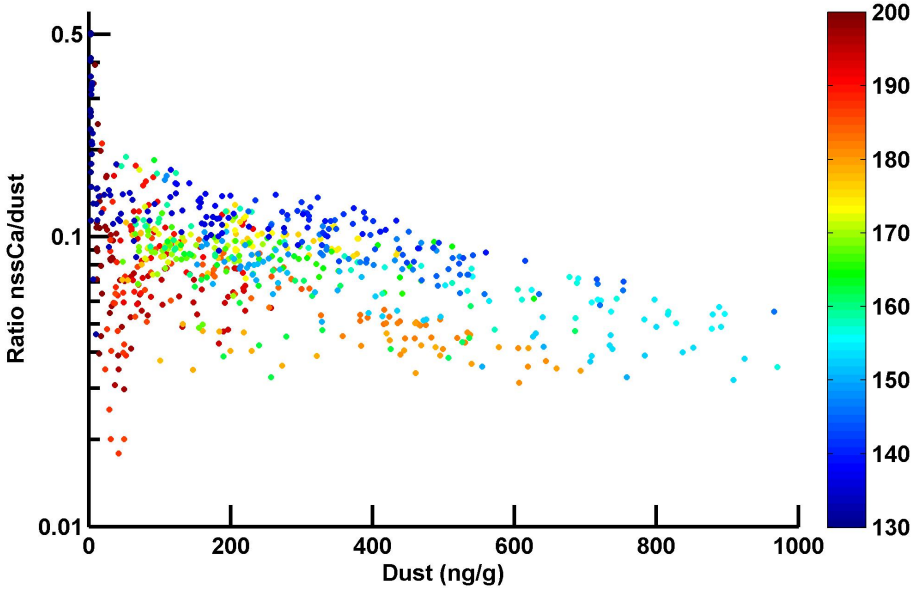

Fig. 6. Scatter plot of the ratio nssCa^{2+}/dust versus dust concentrations using 100 year median data, spanning the time between MIS5.5 and MIS 7.1 (130–200 kyr BP) on logarithmic scales. The colour bar marks the age of the points in kyr BP.

CPD
7, 1113–1137, 2011